Long-Chain Fatty Acid Uptake into Adipocytes Depends on Lipid Raft Function†

Jürgen Pohl,‡ Axel Ring,‡ Robert Ehehalt,‡ Henning Schulze-Bergkamen,‡ Arno Schad,§ Paul Verkade,|| and Wolfgang Stremmel*,‡

Department of Internal Medicine IV, Ruprechts-Karls-University, Heidelberg, Germany, Department of Anatomy, Ruprechts-Karls-University, Heidelberg, Germany, and Max-Planck Institute of Molecular Cell Biology and Genetics, Dresden, Germany

Received September 26, 2003; Revised Manuscript Received December 22, 2003

ABSTRACT: This study investigates the role of lipid rafts and caveolae, a subclass of lipid raft microdomains, in the binding and uptake of long-chain fatty acids (LCFA) by 3T3-L1 cells during differentiation. Disruption of lipid rafts by β-cyclodextrin (βCD) or selective inhibition of caveolae by overexpression of a dominant-negative mutant of caveolin-3 (Cav^{DGV}) resulted in disassembly of caveolae structures at the cell surface, as assessed by electron microscopy. While in 3T3-L1 fibroblasts, which express few caveolae, Cav^{DGV} or βCD had no effect on LCFA uptake, in 3T3-L1 adipocytes the same treatments decreased the level of [^{3}H]oleic acid uptake by up to 55 ± 8 and 49 ± 7%, respectively. In contrast, cholesterol loading of 3T3-L1 adipocytes resulted in a 4-fold increase in the extent of caveolin-1 expression and a 1.7-fold increase in the level of LCFA uptake. Both the inhibitory and enhancing effects of these treatments were constantly increasing with the [^{3}H]oleic acid incubation time up to 5 min. Incubation of 3T3-L1 adipocytes with [^{3}H]stearate followed by isolation of a caveolin-1 positive detergent-resistant membrane (DRM) fraction revealed that [^{3}H]stearate binds to caveolae. Fatty acid translocase (FAT/CD36) was found to be present in this DRM fraction as well. Our data thus strongly indicate a critical involvement of lipid rafts in the binding and uptake of LCFA into 3T3-L1 adipocytes. Furthermore, our findings suggest that caveolae play a pivotal role in lipid raft-dependent LCFA uptake. This transport mechanism is induced in conjunction with cell differentiation and might be mediated by FAT/CD36.

Long-chain fatty acids (LCFA)[1] represent major energy-providing substrates for the human body and are involved in a variety of cellular processes, including membrane synthesis, transcriptional regulation, and intracellular signaling (*1*, *2*). Given these roles, control of their intracellular concentrations through careful regulation of their cellular uptake and efflux is a necessity. Cellular uptake of LCFA occurs by both a saturable mechanism that might be carrier-mediated and a nonsaturable mechanism representing passive flip-flop (*3*). Recent findings imply that lipid rafts might be involved in regulating LCFA uptake (*4*−*7*). Rafts are lateral assemblies of sphingolipids and cholesterol in the plasma membrane that function as platforms to which distinct classes of proteins are specifically associated. On the basis of their particular properties as detergent-resistant membranes, lipid rafts can be isolated from cell lysates (DRMs) (*8*). Caveolae are a subclass of lipid rafts forming characteristic flask-shaped invaginations that can be distinguished by electron microscopy. They represent a specialized membrane domain formed through coalescence of raft domains (*9*) and recruitment of caveolin-1, the major structural protein of caveolae. Caveolae are dynamic structures that can bud from the plasma membrane, forming cytoplasmic vesicles involved both in receptor-mediated uptake of solutes into the cell (*10*) and in transcytosis through the cell (*11*). Although caveolae are found in many cell types, they are especially abundant in adipocytes, where they account for up to 25% of the surface area of the plasma membrane (*12*). In differentiated 3T3-L1 adipocytes, caveolae are often clustered into ringlike arrays (caveolae rosettes) associated with actin filaments, forming a Cav−actin structure (*13*). As 3T3-L1 cells differentiate and acquire the adipocyte phenotype, the number of caveolae increases ∼10-fold (*14*) and the level of protein expression of caveolin-1 increases ∼20-fold (*15*) compared with the values in the undifferentiated fibroblastic state. Therefore, 3T3-L1 adipocytes offer an ideal system for investigating the physiological significance of the lipid raft-mediated LCFA transport system. Another hallmark of differentiation is a dramatic increase in the rate of fatty acid uptake (*16*) accompanied by an increased level of expression of different proteins which have been implicated in fatty acid transport or binding such as $FABP_{PM}$ (plasma membrane fatty acid binding protein) (*17*), FATP1 (fatty acid transport protein) (*18*), fatty acid translocase (FAT/CD36) (*19*), and caveolin-1 (*20*).

† This work was supported by the Deutsche Forschungsgemeinschaft (STR216/11-1), by a Heidelberg University Faculty of Medicine junior scientist grant to J.P. and A.R., and by a Dietmar Hopp Stiftung research grant to W.S.

* To whom correspondence should be addressed: Department of Internal Medicine IV, University Hospital Heidelberg, Bergheimer Str. 58, 69115 Heidelberg, Germany. Telephone: +49-6221-568701. Fax: +49-6221-564116. E-mail: wolfgang.stremmel@med.uni-heidelberg.de.

‡ Department of Internal Medicine IV, Ruprechts-Karls-University.

§ Department of Anatomy, Ruprechts-Karls-University.

|| Max-Planck Institute of Molecular Cell Biology and Genetics.

[1] Abbreviations: βCD, β-cyclodextrin; DRM, detergent-resistant membranes; LCFA, long-chain fatty acids; $FABP_{PM}$, plasma membrane fatty acid binding protein; FATP, fatty acid transport protein; FAT/CD36, fatty acid translocase.

10.1021/bi035743m CCC: $27.50
Published on Web 03/17/2004

Whereas it is not known if FATP-1 or $FABP_{PM}$ is located in a specific plasma membrane microdomain, several reports suggest that in some tissues FAT/CD36 is colocalized with caveolin-1 and resides within caveolae (*7*, *21*). Caveolin-1 was identified as a major plasma membrane fatty acid binding protein in adipocytes that can saturably bind LCFA with high affinity (*20*). Furthermore, caveolin-1 has a well-characterized function in the transport of cholesterol to the cell surface (*22*), and protein expression was shown to be regulated by cholesterol levels (*23*). Caveolae morphology and function critically depend on a sufficient level of cholesterol in the plasma membrane (*11*). Therefore, to inhibit caveolae function, many previous investigators employed cyclodextrin which is known to deplete the plasma membrane from cholesterol (*11*, *24*, *25*). However, besides caveolae, cyclodextrin might also inhibit other lipid raft microdomains. Very recently, Pol and co-workers (*26*) reported a new and specific tool for inhibiting caveolae formation and function. It was shown that deletion of the N-terminus of caveolin-3 results in a dominant-negative protein (termed Cav^{DGV}) that, when overexpressed, prevents the formation of the large caveolin-1−caveolin-2 hetero-oligomeric complexes and leads to the intracellular retention of caveolin-2 and the disappearance of caveolae in MDCK cells (*27*).

In this study, we investigated the role of lipid rafts in the uptake of LCFA in 3T3-L1 cells by modification of cellular cholesterol content, by overexpression of the dominant-negative caveolin-3 mutant Cav^{DGV}, and by disruption of the Cav−actin structure by actin-depolymerizing agents. Furthermore, we studied binding of LCFA to caveolin-1 positive DRM fractions and localization of FAT/CD36 to these fractions.

MATERIALS AND METHODS

[^{3}H]Oleic acid, [^{3}H]stearate, and [^{14}C]octanoic acid were purchased from Biotrend (Cologne, Germany). Fatty acid-free BSA (fraction V), β-cyclodextrin, methyl-β-cyclodextrin, dexamethasone, phloretin, EGTA, leupeptin, pepstatin, chymostatin, and nonradioactive oleic acid and stearate were purchased from Sigma Chemical Co. (St. Louis, MO). Ultima-Gold scintillation fluid was purchased from Packard (Groningen, The Netherlands). 3-Isobutyl-1-methylxanthin, latrunculin A, and cytochalasin were from Calbiochem (Bad Soden, Germany). The mouse antibody against the human transferrin receptor was from Zymed. The antibody against caveolin-1 was from BD Transduction (Heidelberg, Germany), and the antibodies against FAT/CD36 and β-actin were from Santa Cruz Biotechnology (Santa Cruz, CA). The rabbit polyclonal antibody against hemagglutinin (HA) was a kind gift from T. Nilsson (EMBL, Heidelberg, Germany).

Cell Culture. 3T3-L1 fibroblasts were obtained from the American Type Culture Collection (Rockville, MD) and cultured in Dulbecco's modified Eagle's medium (DMEM) supplemented with 10% (v/v) fetal bovine serum (FCS, Gibco BRL), 2 mM L-glutamine, 100 units/L penicillin, and 100 μg/L streptomycin at 37 °C in 10% CO_2 and passaged at ~70% confluence. Confluent fibroblasts were induced to differentiate 1 day after reaching confluence by addition of DMEM containing 10% (v/v) FCS, 5 μg/mL insulin, 0.25 mM dexamethasone, 0.5 mM 3-isobutyl-1-methylxanthine, and 100 ng/mL D-biotin. After 72 h, the medium was replaced with fresh FCS and DMEM containing insulin. Adipocytes were refed with FCS and DMEM every 72 h, and utilized for experiments 8−10 days postdifferentiation.

Evaluation of the Viral Vector. An adenovirus encoding a dominant-negative caveolin-3 mutant Cav^{DGV} that was epitope-tagged with a C-terminal HA tag was generated by Lahtinen *et al.* (*27*). Differentiated 3T3-L1 cells were grown in chamber slides and were incubated with the adenovirus with a multiplicity of infection (moi) of 10−200 plaque-forming units/cell in serum-free medium for 4 h at 37 °C, followed by growth in complete medium for 1 day. Afterward, cells were processed for immunofluorescence microscopy and stained with an HA tag. To achieve an infection rate of more than ~70%, we determined the optimal moi value to be ~100. This moi value was used for infection in all subsequent experiments. Infections were performed 1 day prior to functional assays.

Indirect Immunofluorescence. 3T3-L1 adipocytes were washed three times in PBS, fixed in 2% paraformaldehyde, and labeled with antibodies to the HA tag (4 h at a dilution of 1:200 at 4 °C). The Cy-3-conjugated secondary antibody was applied for 2 h at 4 °C diluted 1:500 in 0.05 mmol/L Tris-HCl (pH 7.4).

Electron Microscopy. 3T3-L1 adipocytes on 5 cm diameter plastic dishes were washed and fixed on ice in 0.5% glutaraldehyde in 0.1 M cacodylate buffer (pH 7.4) and subsequently stored in 2% glutaraldehyde. Cells were then washed in buffer, postfixed for 1 h in 1% aqueous reduced osmium, and dehydrated through a graded series of ethanol. Afterward, cells were treated with hydroxypropyl metacrylate (Fluka), embedded in Epon for ultramicrotomy. Sections (50−60 nm) were collected on Carbon-Formvar-coated copper grids and stained with uranyl acetate and lead citrate before electron microscopical analysis. For assessment of the number of caveolae, dishes with an infection frequency of >95% were analyzed.

Uptake Assays for [^{3}H]Oleic Acid, [^{3}H]Stearate, and [^{14}C]-Octanoate. The [^{3}H]oleic acid uptake assays were performed as described previously (*4*) using confluent 3T3-L1 cell monolayers. Briefly, trace amounts of [^{3}H]oleic acid mixed with measured quantities of nonradioactive oleic acid were dissolved in a defatted BSA solution (173 μmol/L) at a ratio of 1; 1.3 mL of the oleate/BSA solution was incubated with each 3T3-L1 cell monolayer in a 5 cm Ø culture dish at 37 °C. The uptake was stopped by removal of the solution followed by addition of 5 mL of an ice-cold stop solution containing 0.5% (w/v) albumin and 200 μM phloretin. The stop solution was discharged after 2 min, and the culture dishes were washed by dipping them six times in ice-cold incubation buffer. NaOH (2 mol/L) was added to lyse the cells, and aliquots of the lysate were used for protein and radioactivity determination. Radioactivity was determined after the addition of 10 mL of Ultima-Gold in a 1217 Rackbeta liquid scintillation counter (LKB-Wallac, Turku, Finland). Uptake of [^{14}C]octanoate and [^{3}H]stearate was investigated under conditions similar to those for [^{3}H]oleate.

Separation of Cellular Lipids by Thin-Layer Chromatography (TLC). The incorporation of [^{3}H]oleate into cellular lipid pools was assessed after incubation with 173 μmol/L [^{3}H]oleate/albumin mixture (1:1 molar ratio) with 3T3-L1 cell monolayers. Following lysis of 3T3-L1 cells with 1 mol/L NaOH, 0.6 mL of the cell lysate was mixed with 5.4

mL of a chloroform/methanol mixture (2:1, v/v) for the extraction of lipids according to the method of Folch *et al.* (*28*). TLC was performed as described by Holehouse *et al.* (*29*) to separate specific classes of lipids. Standards of monoolein, diolein, triolein, cholesteryl oleate, and free oleate were spotted onto silica gel plates at 10 μg per lane. The lipid phase obtained from the 3T3-L1 cell lysates was concentrated under an N_2 stream and spotted over the standards. The plates were developed in a hexane/diethyl ether/acetic acid mixture (80:20:1, v/v/v) to a height of 15 cm. Lipid standards were stained with I_2 vapor. The areas of each lane corresponding to lipid standards were scraped into a scintillation vial for measurement of radioactivity. At least one control lane per plate contained lipid standards and cellular lipid extracts from cells incubated in medium without [^{3}H]oleate. Control lanes were scraped and the contents counted to determine the background radioactivity for each lipid area, and the mean background radioactivity was subtracted from individual lipid areas. The relative distribution of [^{3}H]oleate in specific cellular lipid classes was determined as the [lipid area (counts per minute) − mean backgroud (counts per minute)]/(sum of counts per minute per lane).

Semiquantitative Measurement of the Level of 12-NBD Stearate Uptake Using Laser Scanning Microscopy (LSM). This method was performed exactly as recently described by us in detail (*4*). Briefly, slides with cultured 3T3-L1 adipocyte monolayers were placed on the stage of an upright LSM 310 microscope (Zeiss, Oberkochen, Germany) and superfused with HEPES-buffered saline [135 mmol/L NaCl, 5 mmol/L KCl, 0.8 mmol/L $MgSO_4$, 0.12 mmol/L $CaCl_2$, 0.8 mmol/L Na_2HPO_4, 10 mmol/L HEPES (pH 7.4), and 5 mmol/L glucose] containing 12-NBD stearate (23 μmol/L) and albumin (173 μmol) at a rate of 40 mL/min. Individual 3T3-L1 adipocytes were identified with a 40× Plan-Neofluar multi-immersion objective lens (numerical aperture of 0.9) (Zeiss) by conventional light microscopy. The system was then switched to the frame mode, and a confocal picture was generated with the 488 nm line of the argon laser (attenuation of 10) for uptake studies with 12-NBD stearate. The emission light was recorded with a photomultiplier after passing through a 525−565 nm band-pass filter under manual gain and black level control. After incubation for 5 min, the fluorescence intensity in a "region of interest" within the cytosol was recorded as arbitrary units, with zero units being the background fluorescence of HEPES-buffered saline.

Manipulation of Cellular Cholesterol Content. Cellular cholesterol content can be modulated by treatment with MβCD−cholesterol complexes at various molar ratios, resulting in either cholesterol enrichment or depletion. Cholesterol loading of mature 3T3-L1 adipocytes with a 5 mM MβCD−cholesterol solution with a molar ratio of 8:1 or 16:1 was carried out as described by Christian *et al.* (*30*). In brief, solutions with different concentrations of MβCD in DMEM were stirred at 37 °C overnight with cholesterol, and then filtered through a 0.45 μm filter (Millipore, Bedford, MA) to remove cholesterol crystals. 3T3-L1 adipocytes in tissue culture dishes were incubated with 2 mL of MβCD−cholesterol complexes for different time intervals in DMEM at 37 °C. At each time point, monolayers were washed three times with DMEM and thereafter used for [^{3}H]oleate uptake assays.

To quantify the uptake of cholesterol, trace amounts of [^{3}H]cholesterol were added for the indicated lengths of time. Lipids were extracted from washed cell monolayers using 2-propanol as previously described (*31*), and the amount of [^{3}H]cholesterol incorporated into cells was determined by liquid scintillation counting. The quantitation of the incorporated cholesterol mass from the MβCD−cholesterol complexes was calculated on the basis of the specific activity of the cholesterol in the complex.

Isolation of Detergent-Resistant Membranes. Detergent extraction with CHAPS was performed as described previously (*32*). 3T3-L1 cells grown in five 225 cm^2 tissue culture flasks were rinsed with ice-cold PBS and scraped on ice into 300 μL of 25 mM Tris-HCl (pH 7.4), 150 mM NaCl, 3 mM EDTA (TNE) buffer containing leupeptin, pepstatin, chymostatin, and antipain (each at 25 μg/mL). Cells were homogenized 15 times through a 22 gauge needle followed by 10 strokes with a tight fitting Dounce homogenizer. The lysate was centrifuged for 5 min at 3000 rpm to obtain a postnuclear supernatant, which was subjected to extraction with 20 mM CHAPS in TNE buffer on ice. The extracts were adjusted to 40% sucrose and overlaid with a discontinuous sucrose gradient (6 mL of 30% sucrose in TNE or 2 mL of TNE without sucrose). The gradients were centrifuged at 200000*g* in a Beckman SW41 rotor for 16−22 h at 4 °C. Fractions (1 mL each) were obtained and used for liquid scintillation counting and Western blotting.

Western Blot Analysis. 3T3-L1 cells were lysed in 50 mmol/L Tris-HCl (pH 7.4) containing 1% Triton X-100, 150 mmol/L EDTA, and antiproteases (1 mmol/L PMSF, 1 μg/mL pepstatin, and 1 μg/mL leupeptin). The protein concentration was quantified by the Bradford procedure (Bio-Rad). Fifty micrograms of total cell protein lysate was separated by 12% SDS−polyacrylamide gel electrophoresis (SDS−PAGE) and transferred to nitrocellulose membranes. Ponceau-S staining was used to confirm equal loading. The origin of the antibodies is specified in Materials and Methods. Antibody binding was visualized using the ECL reagents (Amersham).

RESULTS

βCD and Cav^{DGV} Inhibit the Formation of Caveolae in 3T3-L1 Cells. To study the significance of lipid rafts for LCFA uptake, we used two inhibitors of lipid raft function: βCD and the dominant-negative mutant of caveolin-3 designated Cav^{DGV}. The effects of both inhibitors on caveolae morphology in differentiated 3T3-L1 cells were assessed by electron microscopy (Figure 1A−D), in which caveolae were recognized by their 50−80 nm flask-shaped structure as described previously (*8*). βCD is a sterol-binding agent known to disassemble adipocyte caveolae by cholesterol depletion of the plasma membrane (*24*). While in control cells caveolae associated with the cell surface were found in abundance (Figure 1A,B), βCD treatment (10 mM for 30 min at 37 °C) resulted in the total loss of morphological recognizable invaginated caveolae (Figure 1C). Overexpression of Cav^{DGV} is a recently described tool for selective inhibition of caveolae formation. Figure 1D shows that overexpression of Cav^{DGV} via an adenovirus system markedly diminished the overall number of caveolae at the cell surface of 3T3-L1 cells. However, some segments of the surface with

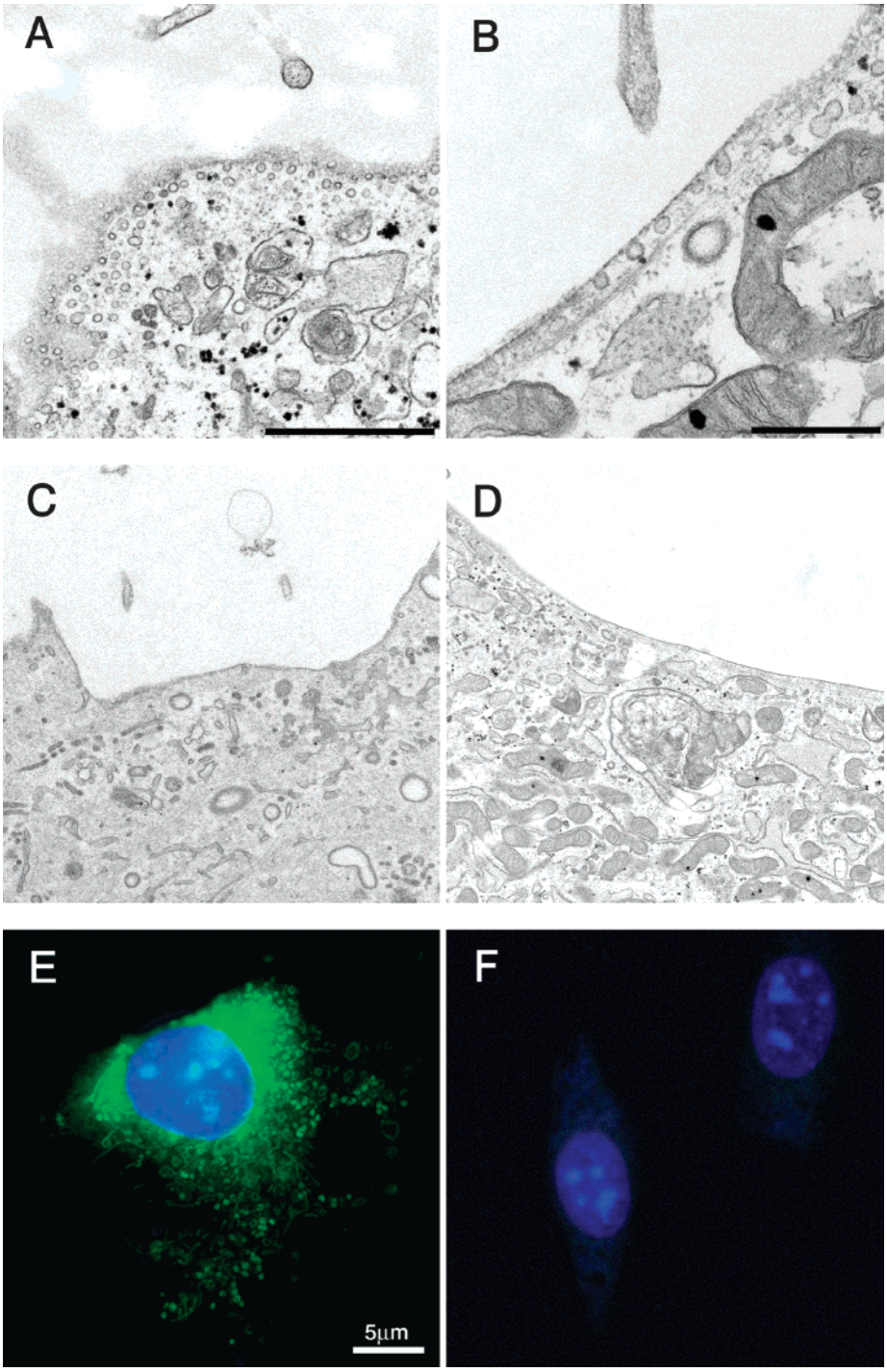

FIGURE 1: Loss of caveolae in cholesterol-depleted 3T3-L1 cells. (A−D) Representative surface segments of 3T3-L1 adipocytes analyzed by electron microscopy. Control cells (A and B) show numerous invaginations on the cell surface. Panel A represents an oblique cut of the cell surface. Panel B shows the ultrastructure of caveolae with the typical bulb shape and characteristic size. In contrast, cells treated with βCD (10 mM for 40 min at 37 °C) (C) demonstrate the disappearance of caveolae. Panel D shows a representative surface of cells treated with Cav^{DGV}. The number of caveolae was markedly diminished. The scale bar represents 1 μm in panels A, C, and D and 0.5 μm in panel B. Indirect immunofluorescence with anti-HA antibodies revealed that HA-tagged Cav^{DGV} was mainly located on spherical structures in the perinuclear region (E). Panel F shows a control that was stained for the HA tag without prior infection by adenovirus. No specific signal can be detected.

normal morphology of caveolae could still be detected. Immunostaining with antibodies to the HA tag demonstrated that ~85% of the cells expressed Cav^{DGV}. Cav^{DGV} was mainly located on spherical structures in the perinuclear region (Figure 1E), a pattern similar to previous reports demonstrating Cav^{DGV} on the membrane of perinuclear lipid droplets and the Golgi complex in BHK cells (*26*) and MDCK cells (*27*). Figure 1F shows a control that was stained for the HA tag without prior infection by the adenovirus. No specific signal could be detected.

Effect of Inhibitors of Lipid Raft Function on LCFA Uptake. In immature 3T3-L1 fibroblasts, the time dependence of [^{3}H]oleate uptake revealed a nearly linear relationship over the course of 10 min (Figure 2A). Inhibition of lipid raft function by βCD (30 min at 10 mmol/L) or Cav^{DGV} had minimal effects on [^{3}H]oleate uptake. In contrast, [^{3}H]oleate

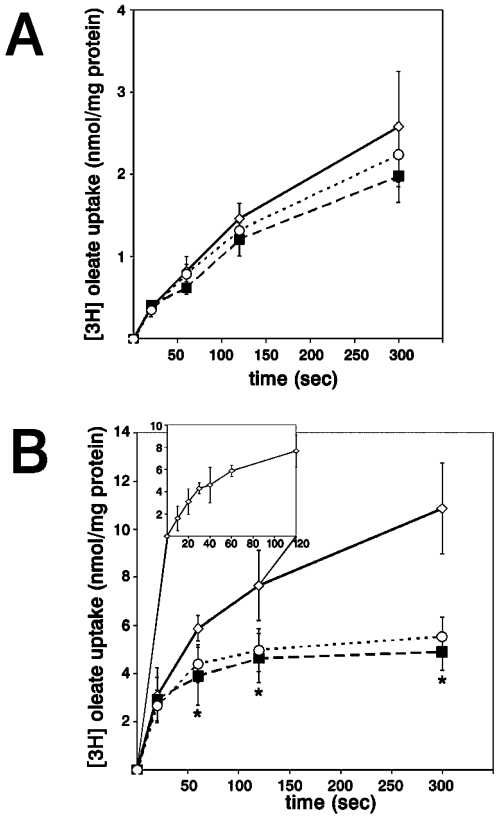

FIGURE 2: Time-dependent effects of lipid raft inhibitors on [^{3}H]-oleate uptake. 3T3-L1 fibroblasts (A) and adipocytes (B) were either not pretreated (◇), pretreated with βCD (10 mM for 50 min at 37 °C) (■), or infected with an adenovirus encoding Cav^{DGV} (○). Afterward, cells were incubated with [^{3}H]oleate for the indicated time, followed by determination of the amount of radioactivity incorporated. Data are means ± the standard deviation of three independent experiments with 10 replicates each.

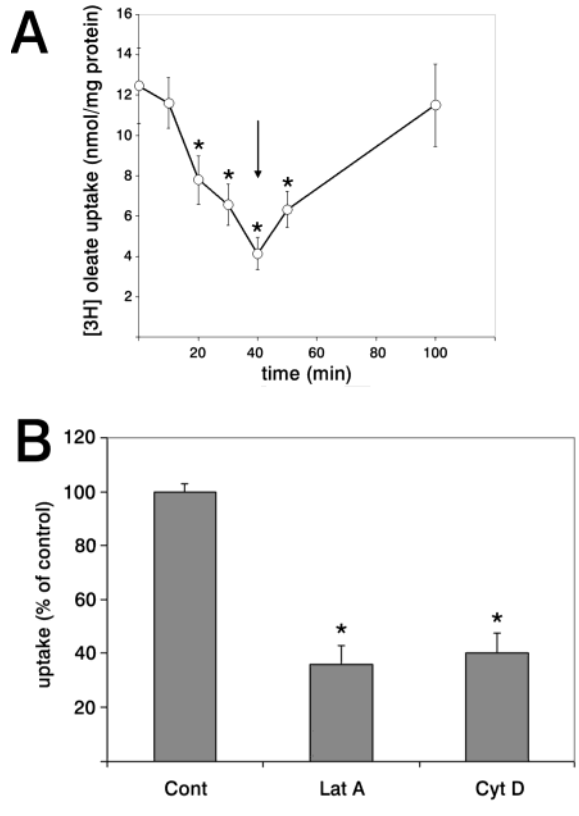

FIGURE 3: Effects of cholesterol manipulation, latrunculin A, and cytochalasin D on uptake of [^{3}H]oleate. (A) Differentiated 3T3-L1 cells were pretreated with βCD for the time periods indicated on the *x* axis followed by determination of the level of [^{3}H]oleic acid accumulation over the course of 5 min. To test the reversibility of the inhibition, cells were washed and replenished with medium containing the MβCD−cholesterol structure (5 mM, 8:1 molar ratio) at the time point denoted with the black arrow. (B) Pretreatment of cells with latrunculin A (1 h, 20 μmol) or cytochalasin D (1 h, 1 μmol) resulted in a significant reduction in the rate of [^{3}H]oleate uptake over the course of 5 min. Graphs show the percentage of radioactivity accumulation compared to controls (=100%). The asterisks indicate statistical significance ($P < 0.05$).

uptake was appreciably faster in fully differentiated 3T3-L1 adipocytes than in fibroblasts (Figure 2B). The time course of [^{3}H]oleate uptake at a concentration of 173 μmol/L was linear over the course of 40 s, representing initial influx and decreased influx thereafter (inset of Figure 2). Unlike in fibroblasts, cholesterol depletion in mature adipocytes reduced the rate of uptake of [^{3}H]oleate in a time-dependent manner; while uptake was only minimally affected in the early (<1 min) uptake phase, in the 5 min incubation experiments it was reduced to 45 ± 7 and 51 ± 7% of control values by βCD and Cav^{DGV}, respectively (Figure 2B). To test the reversibility of the βCD effects, βCD-treated 3T3-L1 adipocyte monolayers were replenished with cholesterol by incubation with MβCD−cholesterol complexes (5 mM, 8:1 molar ratio) for different periods of time. Figure 3A shows that (a) the inhibitory effect of cholesterol depletion was dependent on the duration of preincubation with βCD and (b) cholesterol loading resulted in restoration of normal [^{3}H]oleic acid uptake levels in 3T3-L1 adipocytes.

To investigate if βCD does reduce the rate of uptake of not only oleate but also other LCFA, we investigated the uptake of [^{3}H]stearic acid after βCD preincubation and found a 44.0% reduction of the rate of uptake over the course of 5 min [82.8 ± 15.5 pmol (mg of protein)$^{-1}$ min^{-1} in the βCD-treated cells compared to 147.9 ± 30.9 pmol (mg of protein)$^{-1}$ min^{-1} in the controls ($p < 0.01$)] after incubation for 5 min. However, the effect of βCD treatment was selective for LCFA since it had no effect on the uptake of [^{14}C]octanoate (0.56 ± 0.1 nmol/mg of protein in βCD-treated cells vs 0.5 ± 0.06 nmol/mg of protein in controls), a medium-chain fatty acid believed to enter cells by mechanisms different from those that are operational in the uptake of free fatty acids with a chain length of more than 11 carbons (*33*). Caveolar internalization is dependent on actin (*34*). While βCD disrupts both lipid rafts and Cav−actin structures, actin-depolymerizing agents such as latrunculin A and cytochalasin D are known to selectively disrupt the Cav−actin structure without significantly affecting the organization of caveolae in 3T3-L1 adipocytes (*13*). Latrunculin A (1 h, 20 μmol) and cytochalasin D (1 h, 1 μmol) reduced the rate of late phase [^{3}H]oleate uptake to 35.7 ± 7.4 and 40.4 ± 7.3% of the control value, respectively (Figure 3B).

These results show that in differentiated 3T3-L1 adipocytes lipid rafts constitute an uptake pathway that is dependent on the actin cytoskeleton and is specific for LCFA and predominantly active in the late phase of uptake. Thus, we focused on 5 min incubation experiments to further characterize this lipid raft-mediated LCFA uptake mechanism.

Intracellular Metabolism of [^{3}H]Oleate. Since cellular uptake of substrates can be regulated by intracellular

Table 1: Intracellular Metabolism of [^{3}H]Oleate[a]

	control (counts/mg of protein) (%)	βCD (counts/mg of protein) (%)	Cav^{DGV} (counts/mg of protein) (%)
total counts	38020 ± 4580 (100 ± 11.9)	17348 ± 1387 (100 ± 8.1)	21428 ± 1628 (100 ± 7.6)
free oleate ($R_f = 0.30$)	1824 ± 458 (4.8 ± 1.2)	537 ± 433 (3.1 ± 2.5)	1264 ± 686 (5.9 ± 3.2)
monoolein ($R_f = 0.03$)	7033 ± 3916 (18.5 ± 10.3)	1734 ± 1405 (10.0 ± 8.1)	4371 ± 121 (20.4 ± 8.5)
diolein ($R_f = 0.20$)	8896 ± 1939 (23.4 ± 5.1)	4857 ± 1769 (28.1 ± 10.2)	4735 ± 2185 (22.1 ± 10.2)
triolein ($R_f = 0.73$)	11253 ± 5703 (29.6 ± 15.0)	6418 ± 2151 (37.0 ± 12.4)	6642 ± 1907 (31.0 ± 8.9)
cholesteryl ester ($R_f = 0.87$)	6273 ± 2129 (16.5 ± 5.6)	1543 ± 1075 (8.9 ± 6.2)	2635 ± 1864 (12.3 ± 8.7)
unidentified	2737 ± 2243 (7.2 ± 5.9)	2255 ± 1509 (13.0 ± 8.7)	1778 ± 1371 (8.3 ± 6.4)

[a] To investigate LCFA metabolism in control cells and cells treated with βCD or Cav^{DGV}, 3T3-L1 cell monolayers were incubated in serum-free medium with 173 μmol/L oleate with [^{3}H]oleate tracer bound to 173 μmol/L albumin for 5 min. 3T3-L1 cells were lysed followed by extraction of the lysate according to the method of Folch *et al.* (*28*). The lipid phase was separated by TLC using hexane, diethyl ether, and acetic acid (80:20:1, v/v/v) as the developing solvent. Areas of the TLC plates corresponding to lipid standards were removed for scintillation counting. All spots were counted, and the counts were totaled. The percentage of [^{3}H]oleate in lipid classes was calculated as (lipid area counts per minute − mean background counts per minute)/(sum of counts per minute per lane). Since the solvent front was allowed to reach the upper edge of the TLC plate, the t_R values were calculated using the distance from the origin to the upper edge of the plate as the denominator. Data are means ± standard deviations of five replicate experiments.

metabolism, it is theoretically conceivable that βCD and Cav^{DGV} might exert their inhibitory effects on intracellular LCFA accumulation by interference with LCFA metabolism, e.g., by preventing esterification. Therefore, we analyzed the cellular fate of incorporated fatty acid and found that in lysates from control cells or cells treated with either βCD or Cav^{DGV} more than 90% were recovered metabolized to various lipid derivatives within the first 5 min of the incubation (Table 1). The relative amount of radioactively labeled monoolein, diolein, triolein, cholesteryl oleate, and free oleate was comparable in controls and treated cells. To further rule out interference of lipid raft inhibitors on LCFA metabolization, we assessed the uptake of 12-NBD stearate, a fluorescent LCFA derivative that is not metabolized (*4*, *35*). We previously described a semiquantitative, LSM-based method of visualizing and quantifying the uptake of 12-NBD stearate on a subcellular level. Here we used this method to measure fluorescence intensity in a previously defined cytosolic region of interest in a single cell as arbitrary units after incubation for 5 min. Following pretreatment with βCD or Cav^{DGV}, the rate of uptake of 12-NBD stearate into adipocytes was decreased to 46.8 ± 9.1 and 55 ± 8.9% of control levels, respectively. Therefore, the nonmetabolizable fatty acid derivative 12-NBD stearate is inhibited to a degree similar to that of native [^{3}H]oleic acid and [^{3}H]stearic acid. Given these results, it appears that βCD or Cav^{DGV} does not interfere with the intracellular metabolism of fatty acids.

Cholesterol Loading Stimulates [^{3}H]Oleate Uptake. To further investigate the association of cellular cholesterol content with LCFA uptake, we performed cholesterol loading of 3T3-L1 adipocytes. 3T3-L1 adipocytes were pretreated with MβCD−cholesterol complexes at molar ratios of either 8:1 or 16:1 containing trace amounts of [^{3}H]cholesterol. Cells treated with either solution became enriched with radiolabeled cholesterol over time, but this effect was significantly more pronounced after treatment with the 8:1 ratio (Figure 4A). Western blot analysis and densitometric scanning revealed that incubation with MβCD−cholesterol complexes resulted in a 4-fold increase in the level of caveolin-1 expression that paralleled the degree of cholesterol accumulation (Figure 4B). In further experiments, we measured the rate of [^{3}H]oleate uptake after pretreatment of cells with nonradioactive cholesterol loading solutions (Figure 4C). While there was no influence on [^{3}H]oleate uptake in the 20 s experiments, after incubation for 5 min we observed a significant increase in the rate of [^{3}H]oleate uptake in cells pretreated for 6 h with a MβCD−cholesterol solution at a molar ratio of 8:1 and, to a lesser degree, of 16:1.

Binding of [^{3}H]Stearate to Detergent-Resistant Membranes. One possible explanation for the observation that disruption of caveolae results in a diminished level of LCFA accumulation is that LCFA uptake might involve direct binding of LCFA to lipid raft membrane constituents. To further investigate this possibility, we isolated DRMs by CHAPS extraction using differentiated 3T3-L1 adipocytes preincubated with [^{3}H]stearic acid. Following CHAPS treatment of postnuclear supernatants and sucrose density gradient centrifugation, the DRMs float to the low-density membrane fraction in a cholesterol-dependent manner. Therefore, besides caveolae, DRM fractions include all different kinds of lipid raft microdomains. As shown in Figure 5A, caveolin-1 was exclusively located in the upper (DRM) fractions, while the transferrin receptor (a marker protein of detergent-soluble membranes) was present in only the lower fractions. Pretreatment with βCD resulted in a nearly complete abolishment of the buoyant fraction and displacement of the caveolin-1 peak into fractions 2−6 (data not shown).

Figure 5B shows the distribution of [^{3}H]stearic acid over the different sucrose gradient fractions. A peak of radioactivity in the DRM fraction suggests that [^{3}H]stearic acid indeed binds to lipid rafts. As expected, this association was lost when cells had been pretreated with βCD prior to incubation with [^{3}H]stearic acid.

Association of FAT/CD36 with DRMs. To further investigate the role of lipid rafts in LCFA uptake, we studied the subcellular expression of FAT/CD36 in 3T3-L1 adipocytes. Figure 6 shows that FAT/D36 is expressed in caveolin-1-enriched fraction 11 (compare Figure 5) as well as in the non-lipid raft fractions. However, our results do not differentiate between plasma membrane and endomembrane expression in either the lipid raft- or detergent-soluble membrane fraction.

DISCUSSION

We recently reported that lipid rafts are involved in LCFA uptake and intracellular trafficking of HepG2 hepatoma cells (*4*) and human microvascular endothelial cells (*5*). 3T3-L1 cells seemed to be an ideal model for further investigating this new concept of LCFA uptake. We reasoned that if a

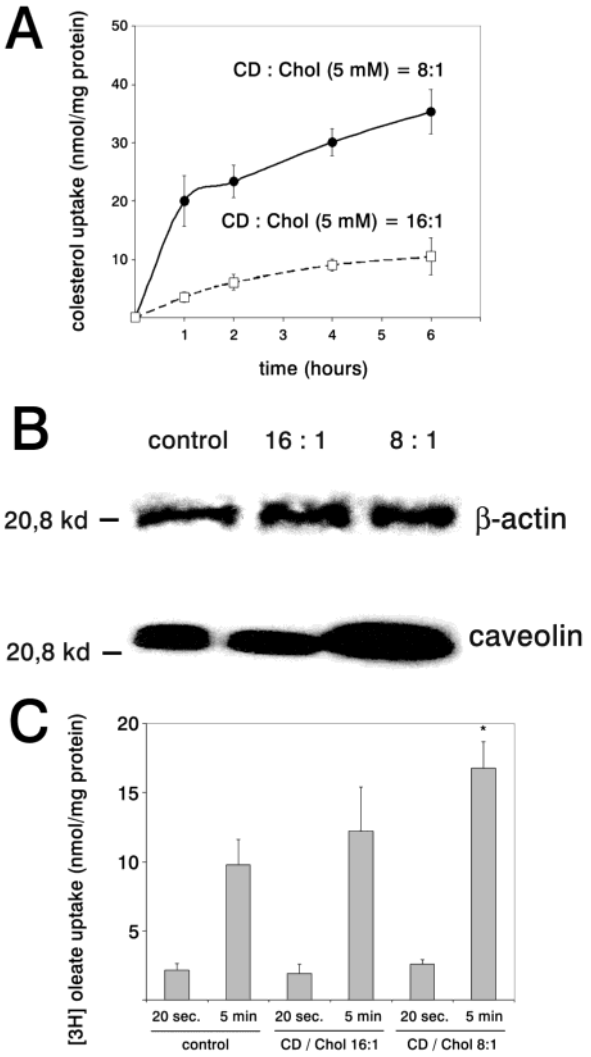

FIGURE 4: Cholesterol loading of 3T3-L1 adipocytes. Panel A shows [^{3}H]cholesterol accumulation in 3T3-L1 adipocytes. Cells were incubated with [^{3}H]cholesterol complexes of MβCD (5 mM) with a molar ratio of either 8:1 (●) or 16:1 (□) for a total of 6 h. At each time point, the amount of incorporated cholesterol from the MβCD−cholesterol complexes was calculated on the basis of the specific activity of [^{3}H]cholesterol in the complex. (B) Western blot analysis revealed that incubation with [^{3}H]cholesterol−MβCD complexes was paralleled by significant induction of caveolin-1 expression that correlated with the degree of cholesterol accumulation. In contrast, levels of β-actin were not affected by this treatment. A total of 20 μg of protein was applied per lane. Panel C shows incorporation of [^{3}H]oleate in control cells and in 3T3-L1 adipocytes that were exposed to cholesterol loading with the indicated molar ratios of MβCD−cholesterol complexes. Data in panels A and C are means ± the standard deviation of three experiments with eight replicates each. The asterisks indicate statistical significance ($P < 0.05$).

lipid raft-mediated LCFA uptake mechanism existed, it was likely to be strongly induced in 3T3-L1 adipocytes differentiating according to a program which maximizes cavelae expression as well as LCFA accumulation. This study represents the first biochemical description of a novel LCFA uptake pathway that is induced during adipocyte differentiation and involves lipid rafts. The experimental evidence is based on both modulation of lipid raft function and labeling of a caveolin-1 positive DRMs fraction by radioactive stearate.

Removal of cholesterol from the plasma membrane by βCD and overexpression of Cav^{DGV} resulted in disassembly

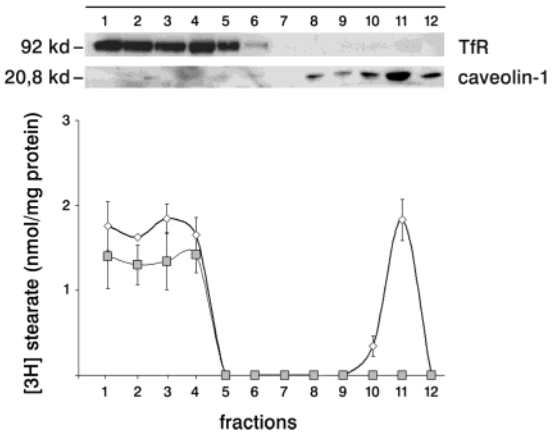

FIGURE 5: Isolation of a lipid raft-enriched membrane fraction. (A) CHAPS-insoluble lipid rafts were separated from soluble membranes on sucrose gradients and immunoblotted with antibodies to the transferring receptor (TfR) or caveolin-1. A peak of caveolin-1 was detected in fractions 8−11 of the gradient, while the peak of the transferring receptor, representing the majority of the cell membranes, was detected in fractions 1−5. Representative blots from six separate experiments are shown. (B) Binding of [^{3}H]stearic acid to lipid rafts. After incubation for 5 min with [^{3}H]stearic acid, differentiated 3T3-L1 cells were exposed to an ice-cold stop solution containing 0.5% (w/v) albumin and 200 μM phloretin. Afterward, cells were lysed, and CHAPS-insoluble lipid rafts were separated from soluble membranes on sucrose gradients. The amount of radioactivity associated with the fractions was determined (◇). There was a peak of radioactivity cofractionating with caveolin-1, indicating binding to lipid rafts. This peak was lost when cells were incubated with βCD prior to [^{3}H]stearic acid incubation (□). Data are means ± the standard deviation of three independent experiments with 10 replicates each.

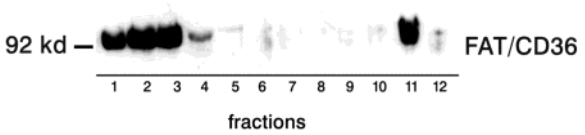

FIGURE 6: Western blot analysis of FAT/CD36. Typical results of the Western blot analysis of DRMs isolated from 3T3-L1 adipocytes are shown. FAT/CD36 is present in caveolin-1-enriched fraction 11 (see Figure 5).

of caveolae structures and a time-dependent reduction of oleate and stearate incorporation, while uptake of octanoate was not affected. These findings suggest a lipid raft-mediated uptake mechanism that is selective for LCFA and operational predominantly in the later uptake phase. Furthermore, since Cav^{DGV} overexpression specifically blocks caveolae, our results suggest that caveolae play a pivotal role in this lipid raft-mediated pathway. However, complete disruption of the lipid raft structure was not necessary for inhibition of LCFA uptake since an inhibitory effect of the same magnitude was afforded by disrupting the Cav−actin structure using actin-depolymerizing agents, which do not interfere with the DRM membrane structure (*13*). Therefore, we assume that the DRM function pertinent to LCFA uptake is at least in part associated with the filamentous actin cytoskeleton. Modulation of LCFA metabolism by inhibitors of lipid raft function is not likely to interfere with LCFA uptake in our experimental system since accumulation of the nonmetabolizable fatty acid derivative 12-NBD stearate occurred to a degree comparable to the degree of inhibition of native fatty acids. Furthermore, esterification of LCFA was not hampered by treatment with inhibitors. While in 3T3-L1 adipocytes

cholesterol depletion resulted in a decreased rate of LCFA uptake, loading cells with cholesterol increased the level of LCFA accumulation in the later uptake phase and was paralleled by strong induction of caveolin-1 expression. This is in line with findings of previous investigators, who found that caveolin-1 expression is under positive control of cellular cholesterol levels (*23*) and that caveolin-1 expression in cholesterol-loaded cells drives caveolae formation (*36*). The importance of cellular cholesterol content and lipid raft function for LCFA uptake has been suggested by Kolleck *et al.* (*7*), who demonstrated that in type II pneumocytes cholesterol loading induces formation of caveolae-like microdomains in the surface membrane and stimulates uptake of palmitate. The involvement of caveolae in LCFA uptake *in vivo* is supported by the data recently reported by Razani and co-workers (*6*), who showed that caveolin-1 deficient mice demonstrate a loss of caveolae and develop severely elevated triglyceride and free fatty acid levels. Furthermore, mutant mice exhibit overt resistance to diet-induced obesity, and histologically, adipocytes have smaller lipid droplets. This indicates that the lack of caveolin-1 results in the loss of caveolae and defects in LCFA uptake or regulation.

However, the exact mechanism of lipid raft-mediated uptake is not known. Our results show that LCFA directly bind to DRMs and that FAT/CD36, a major LCFA uptake protein of adipocytes (*19*), is expressed in DRMs. This finding is in line with recent reports about type II pneumocytes (*7*) and HEK-293T cells (*21*), where FAT/CD36 was shown to reside in DRM fractions. When stimulated, FAT/CD36 can translocate from an intracellular depot to the plasma membrane (*37*) and enhance LCFA uptake in adipocytes (*19*). We at present are investigating if FAT/CD36 is localized in intracellular nonraft depots, from where it might be translocated to lipid rafts at the plasma membrane level upon stimulation.

On the basis of our data, we propose that at least two distinct pathways of LCFA uptake coexist in 3T3-L1 adipocytes: (a) a rapid, lipid raft-independent mechanism that is operational predominantly in the first minute of uptake and (b) a slower, lipid raft-mediated route that becomes predominant over time. The early and rapid mechanism most probably represents a carrier-mediated high-affinity but low-capacity transport that might be facilitated by a classical fatty acid transport protein of the plasma membrane. There are at least two alternative mechanisms that could contribute to the crucial role of lipid rafts in the low-affinity and high-capacity LCFA transport pathway uptake.

(1) LCFA might bind to FAT/CD36 or other not yet identified transport proteins that are located in caveolae, followed by actin-dependent internalization of caveolae (*33*). This concept is supported by the finding that LCFA uptake is inhibited by actin-disrupting agents.

Furthermore, since uptake by endocytosis is a relatively slow process, this mechanism could explain why interference with lipid raft function predominantly affects the late uptake phase of LCFA. Although caveolae are probably not involved in constitutive endocytosis (*38*), internalization of these microdomains can be stimulated by binding of specific ligands, e.g., albumin (*39*). This is in line with our previous studies on LCFA uptake in HepG2 cells and microvascular endothelial cells (*4*, *5*) that suggested endocytosis and intracellular transport of LCFA via caveolae. However, in this study, the intracellular movements of LCFA were not investigated.

(2) Alternatively, LCFA might interact with FAT/CD36 or other fatty acid transport or binding proteins that reside in lipid rafts and initiate facilitated transport or passive flip-flop of LCFA across the lipid bilayer. Subsequently, caveolin-1, which is situated at the inner leaflet of the lipid bilayer, might bind LCFA and either act as an intracellular vehicle for LCFA tranport or serve as a buffer that presents LCFA to cytoplasmatic fatty acid binding proteins for further intracellular channeling. Indeed, there is a growing body of evidence of the involvement of caveolin-1 in fatty acid uptake and intracellular trafficking. Caveolin-1 moves from plasma membrane caveolae to lipid droplets in response to free fatty acids (*26*, *40*) and might therefore shuttle LCFA between subcellular membrane compartments. Moreover, recent findings indicate that caveolin-1 plays an important role in CD36/FAT functioning and regulation, since caveolin-1 induces targeting of FAT/CD36 to the plasma membrane (*21*).

In conclusion, our findings strongly support the hypothesis of a lipid raft-dependent LCFA uptake mechanism that is induced in 3T3-L1 cells during differentiation from fibroblasts to adipocytes. This mechanism apparently involves binding of LCFA to lipid rafts, potentially via FAT/CD36. Furthermore, the sensitivity of LCFA uptake to selective inhibition of caveolae by Cav^{DGV} points to a crucial role of this microdomain in the lipid raft-mediated pathway. Since caveolae are involved in insulin signaling and might regulate translocation of GLUT-4 to the cell surface (*24*, *41*), further investigation of caveolae-mediated LCFA uptake may have important consequences for furthering our understanding of the relation between fatty acid metabolism and insulin resistance.

ACKNOWLEDGMENT

We thank Simone Staffer and Sonja Weber for technical assistance and Monika Mews for imaging processing. We are also grateful to Dr. Kai Simons (Max-Planck Institute of Molecular Cell Biology and Genetics) for the generous gift of the caveolin-3 mutant Cav^{DGV}.

REFERENCES

1. Van der Vusse, G. J., Glatz, J. F., Stam, H. C., and Reneman, R. S. (1992) Fatty acid homeostasis in the normoxic and ischemic heart, *Physiol. Rev. 72*, 881−940.
2. Newsholme, E. A., Calder, P., and Yaqoob, P. (1993) The regulatory, informational, and immunomodulatory roles of fat fuels, *Am. J. Clin. Nutr. 57*, 738−750.
3. Stump, D. D., Fan, X., and Berk, P. D. (2001) Oleic acid uptake and binding by rat adipocytes define dual pathways for cellular fatty acid uptake, *J. Lipid Res. 42*, 509−520.
4. Pohl, J., Ring, A., and Stremmel, W. (2002) Uptake of long-chain fatty acids in HepG2 cells involves caveolae: analysis of a novel pathway, *J. Lipid Res. 43*, 1390−1399.
5. Ring, A., Pohl, J., Völkl, A., and Stremmel, W. (2002) Evidence for vesicles that mediate long-chain fatty acid uptake by human microvascular endothelial cells, *J. Lipid Res. 43*, 2095−2104.
6. Razani, B., Combs, T. P., Wang, X. B., Frank, P. G., Park, D. S., Russell, R. G., Li, M., Tand, B., Jelicks, L. A., Scherer, P. E., and Lisanti, M. P. (2002) Caveolin-1-deficient mice are lean, resistant to diet-induced obesity, and show hypertriglyceridemia with adipocyte abnormalities, *J. Biol. Chem. 277*, 8635−8647.
7. Kolleck, I., Guthmann, F., Ladhoff, A. M., Tandon, N. N., Schlame, M., and Rüstow, B. (2002) Cellular cholesterol stimulates uptake of palmitate by redistribution of fatty acid translocase in type II pneumocytes, *Biochemistry 41*, 6369−6375.

8. Parton, R. G., and Simons, K. (1995) Digging into caveolae, *Science 269*, 1398−1399.
9. Simons, K., and Ikonen, E. (1997) Functional rafts in cell membranes, *Nature 387*, 569−572.
10. Anderson, R. G. W., Kamen, B. A., Rothberg, K. G., and Lacey, S. W. (1992) Potocytosis: sequestration and transport of small molecules by caveolae, *Science 255*, 410−411.
11. Schnitzer, J. E., Oh, P., Pinney, E., and Allard, J. (1994) Filipin III-sensitive caveolae-mediated transport in endothelium: reduced transcytosis, scavenger endocytosis, and capillary permeability of select macromolecules, *J. Cell Biol. 127*, 1217−1232.
12. Parton, R. G., Molero, J. C., Floetenmeyer, M., Green, K. M., and James, D. E. (2002) Characterization of a distinct plasma membrane macrodomain in differentiated adipocytes, *J. Biol. Chem. 277*, 46769−46778.
13. Kanzaki, M., and Pessin, J. E. (2002) Caveolin-associated filamentous actin (Cav-actin) defines a novel F-actin structure in adipocytes, *J. Biol. Chem. 277*, 25867−25869.
14. Fan, J. Y., Carpentier, J. L., van Obberghen, E., Grunfeld, C., Gorden, P., and Orci, L. (1983) Morphological changes of the 3T3-L1 fibroblast plasma membrane upon differentiation to the adipocyte form, *J. Cell Sci. 61*, 219−230.
15. Scherer, P. E., Lisanti, M. P., Baldini, G., Sargiacomo, M., Mastick, C. C., and Lodish, H. F. (1994) Induction of caveolin during adipogenesis and association of GLUT4 with caveolin-rich vesicles, *J. Cell Biol. 127*, 1233−1243.
16. Abumrad, N. A., Forest, C. C., Regen, D. M., and Sanders, S. (1991) Increase in membrane uptake of long-chain fatty acids early during preadipocyte differentiation, *Proc. Natl. Acad. Sci. U.S.A. 88*, 6008−6012.
17. Zhou, S. L., Stump, D., Sorrentino, D., Potter, B. J., and Berk, P. D. (1992) Adipocyte differentiation of 3T3-L1 cells involves augmented expression of a 43-kDa plasma membrane fatty acid-binding protein, *J. Biol. Chem. 268*, 14456−14461.
18. Schaffer, J. E., and Lodish, H. F. (1994) Expression cloning and characterization of a novel adipocyte long chain fatty acid transport protein, *Cell 79*, 427−436.
19. Abumrad, N. A., El-Maghrabi, M. R., Amri, E. Z., Lopez, E., and Grimaldi, P. A. (1993) Cloning of rat adipocyte membrane-protein implicated in binding or transport of long chain fatty acids that is induced during preadipocyte differentiation: homology with human CD 36, *J. Biol. Chem. 268*, 17665−17668.
20. Trigatti, B. L., Anderson, R. G. W., and Gerber, G. E. (1999) Identification of caveolin-1 as a fatty acid binding protein, *Biochem. Biophys. Res. Commun. 255*, 34−39.
21. Frank, P. G., Marcel, Y. L., Connelly, M. A., Lublin, D. M., Franklin, V., Williams, D. L., and Lisanti, M. P. (2002) Stabilization of caveolin-1 by cellular cholesterol and scavenger receptor class B type I, *Biochemistry 41*, 11931−11940.
22. Fielding, C. J., and Fielding, P. E. (2001) Caveolae and intracellular trafficking of cholesterol, *Adv. Drug Delivery Rev. 49*, 251−264.
23. Bist, A., Fielding, P. E., and Fielding, C. J. (1997) Two sterol regulatory element-like sequences mediate up-regulation of caveolin gene transcription in response to low-density lipoprotein free cholesterol, *Proc. Natl. Acad. Sci. U.S.A. 94*, 10693−10698.
24. Parpal, S., Karlsson, M., Thorn, H., and Stralfors, P. (2001) Cholesterol depletion disrupts caveolae and insulin receptor signalling for metabolic control via insulin receptor substrate-1, but not for mitogen-activated protein kinase control, *J. Biol. Chem. 276*, 9670−9678.
25. Hailstones, D., Sleer, L. S., Parton, R. G., and Stanley, K. K. (1998) Regulation of caveolin and caveolae by cholesterol in MDCK cells, *J. Lipid Res. 39*, 369−379.
26. Pol, A., Luetterforst, R., Lindsay, M., Heino, S., Ikonen, E., and Parton, R. G. (2001) A caveolin dominant negative mutant associates with lipid bodies and induces intracellular cholesterol imbalance, *J. Cell Biol. 152*, 1057−1070.
27. Lahtinen, U., Honsho, M., Parton, R. G., Simons, K., and Verkade, P. (2003) Involvment of caveolin-2 in caveolar biogenesis in MDCK cells, *FEBS Lett. 538*, 85−88.
28. Folch, J., Lees, M. B., and Stanley, G. H. S. (1957) A simple method for isolation and purification of total lipids from animal tissues, *J. Biol. Chem. 226*, 497−509.
29. Holehouse, E. L., Liu, M. L., and Aponte, G. W. (1998) Oleate distribution in small intestinal epithelial cells expressing intestinal-fatty acid binding protein, *Biochim. Biophys. Acta 390*, 52−64.
30. Christian, A. E., Haynes, M. P., Phillips, M. C., and Rothblat, H. (1997) Use of cyclodextrins for manipulating cellular cholesterol content, *J. Lipid Res. 38*, 2264−2272.
31. McCloskey, H. M., Rothblat, G. H., and Glick, J. M. (1987) Incubation of acetylated low-density lipoprotein with cholesterol-rich dispersions enhances cholesterol uptake by macrophages, *Biochim. Biophys. Acta 921*, 320−332.
32. Fiedler, K., Kobayashi, T., Kurzchalia, T. V., and Simons, K. (1993) Glycoshpingolipid enriched, detergent-insoluble complexes in protein sorting epithelial cells, *Biochemistry 32*, 6365−6373.
33. Stremmel, W. (1988) Uptake of fatty acids by jejunal mucosal cells is mediated by a fatty acid binding membrane protein, *J. Clin. Invest. 82*, 2001−2010.
34. Pelkmans, L., Püntener, D., and Helenius, A. (2002) Local actin polymerization and dynamin recruitment in SV40-induced internalization of caveolae, *Science 296*, 535−539.
35. Elsing, C., Gorski, J., Boecker, C., and Stremmel, W. (1998) Long-chain fatty acid uptake by skeletal myocytes: a confocal laser scanning microscopy study, *Cell. Mol. Life Sci. 54*, 744−750.
36. Li, S., Song, K. S., Koh, S., and Lisanti, M. P. (1996) Baculovirus-based expression of mammalian caveolin in Sf21 insect cells. A model system for the biochemical and morphological study of caveolar biogenesis, *J. Biol. Chem. 271*, 28647−28654.
37. Bonen, A., Luiken, J. J., Arumugam, Y., Glatz, J. F., and Tandon, N. N. (2000) Acute regulation of fatty acid uptake involves the cellular redistribution of fatty acid translocase, *J. Biol. Chem. 275*, 14501−14508.
38. Thomsen, P., Roepstrorff, K., Stahlhut, M., and van Deurs, B. (2002) Caveolae are highly immobile plasma membrane microdomains, which are not involved in constitutive endocytic trafficking, *Mol. Biol. Cell 13*, 238−250.
39. Minshall, R. D., Tiruppathi, C., Vogel, S. M., Niles, W. D., Gilchrist, A., Hamm, H. E., and Malik, A. B. (2000) Endothelial cell-surface gp60 activates vesicle formation, and trafficking via Gi-coupled Src kinase signaling pathway, *J. Cell Biol. 150*, 1057−1069.
40. Ostermeyer, A. G., Paci, J. M., Zeng, Y., Lublin, D. M., Munro, S., and Brown, D. A. (2001) Accumulation of caveolin in the endoplasmic reticulum redirects the protein to lipid storage droplets, *J. Biol. Chem. 276*, 38121−38138.
41. Kanzaki, M., and Pessin, J. E. (2001) Insulin-stimulated GLUT4 translocation in adipocytes is dependent upon cortical actin remodeling, *J. Biol. Chem. 276*, 42436−42444.

BI035743M